6.4 Derivation of EOFs and test on their representativity.

In this section we present the main results related to the EOF derivation, namely the vector modes themselves and the way they manage to approach the data profiles from which they were obtained (described in terms of the variance explained). We also present results for the extent to which shallow profiles (not entering the EOF derivation and reflecting mainly the shelf dynamics) can be expressed in terms of the EOFs (obtained from deep profiles and therefore reflecting mainly the shelf break and offshore dynamics). In this section results will restrict to the three basic variables, that is potential temperature, salinity and density.

We shall present different types of Figures. First, we will show Figures with four frames: the upper two frames correspond to the six leading vector modes; the lower left frame shows the variance explained by each of the modes, and the lower right one shows the accumulated variance (the thicker line being the total variance explained by the six leading modes). It must be taken into account that in this context the “variance” refers to that of the casts used to compute the EOFs (i.e., the deep casts only). Later on we will show equivalent Figures for the total field variance (i.e., including deep and shallow casts), which can differ significantly from the present ones.

We will show results from both the non-standardized analysis (frame (a) including the four frames mentioned above) and from the standardized analysis (frame (b) also containing four frames), in which the covariance matrix elements are normalized by the corresponding level variance (therefore resulting in a correlation matrix). For the first analysis, the layers with the largest variability will obviously dominate the fitting process, whereas the second method is equivalent to assume that the variance is evenly distributed in the vertical.

Since including all Figures corresponding to the three variables and the two types of analyses for each of the campaigns would result in a large number of Figures, we will show a selection of them. Namely, we will focus on FANS III, which correspond to summer conditions, and FANS II, corresponding to winter conditions. Some comments will also be made on FANS I and MEGO 94.

6.4.1 Resulting eigenvectors

6.4.1.1 FANS III – Summer conditions

On average, during summer (or nearly summer) conditions, the vertical structure of temperature is characterized by a well established thermocline under which there is little temperature variability. Consequently, for the non-standardized analysis the EOFs try to fit the dominant levels (in terms of variance), making the percentage of variance explained at lower levels to be rather low, with a noisy shape (see Figure 6-34). For the standardized analyses, the explained variance is significantly higher at low levels, although profiles still have a wavy pattern. The latter is apparently associated to the vector modes crossing the zero value (unlike the Fourier decomposition, the EOFs can cross the zero several times, as in this case for both analyses).

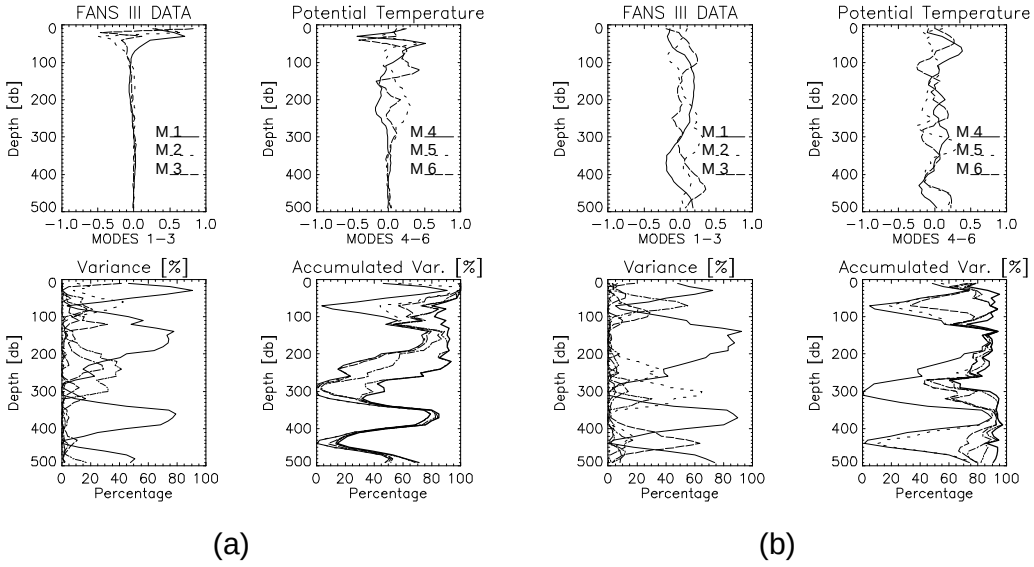

Figure 6-34 FANS III Potential temperature vector modes (6), explained variance and accumulated explained variance for the non-standardized (a) and standardized (b) analyses.

A related difference between the two types of analysis is that the standardized modes have more structure at deep levels, while the non-standardized ones, particularly the first three modes, tend to zero after the first 100 m. For the latter, a large fraction of variance is explained (by the six leading modes) in the upper 200 m, but the fraction is rather low beneath that depth. For the standardized analysis, the fact that the first modes have more structure

in the whole vertical domain results in a more reasonable accumulated variance at all levels.

For the case of salinity (Figure 6-35), the non-standardized analysis fails to reproduce only the lowest 100 m, and variance profiles are much more regular in the vertical. Another difference is that most of the variance can be explained with only two modes, one accounting for the variance of the upper 100 m and the other accounting for the variance of intermediate levels (100-400 m).

A similar behaviour is obtained for the standardized analysis, although in this case the contribution of a third mode is required to explain the variance of the lowest 100 m. On average, the latter model gives better results (in the sense of accounting for a higher fraction of variance), even though the non-standardized gives the best fit between 100 and 250 m.

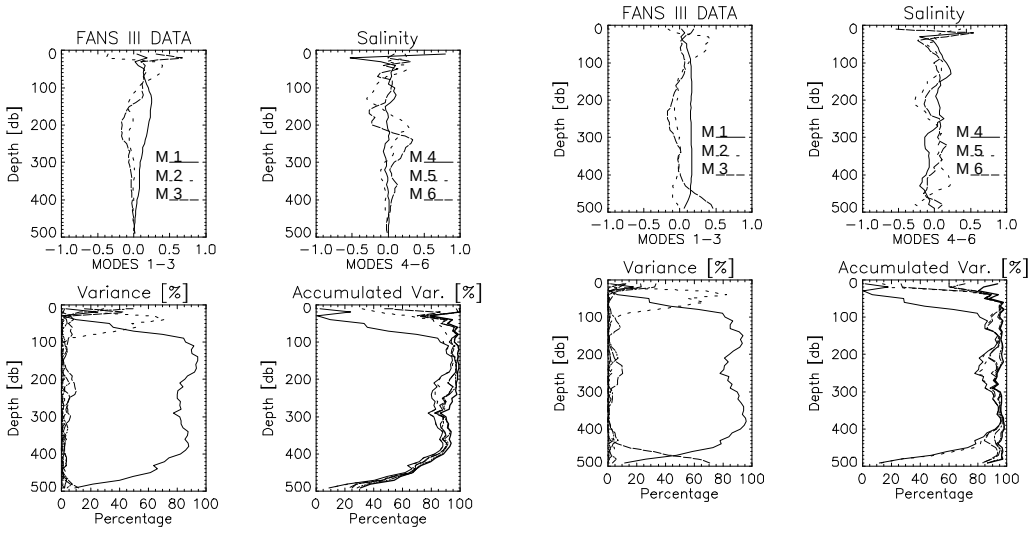

Figure 6-35 FANS III Salinity vector modes (6), explained variance and accumulated explained variance for the non-standardized (a) and standardized (b) analyses.

Finally, the non-standardized analysis applied to FANS III data gives its best results with density, with an explained variance above 85% at all depths (Figure 6-36). Nevertheless, the overall fit with six modes is still better with the standardized analysis.

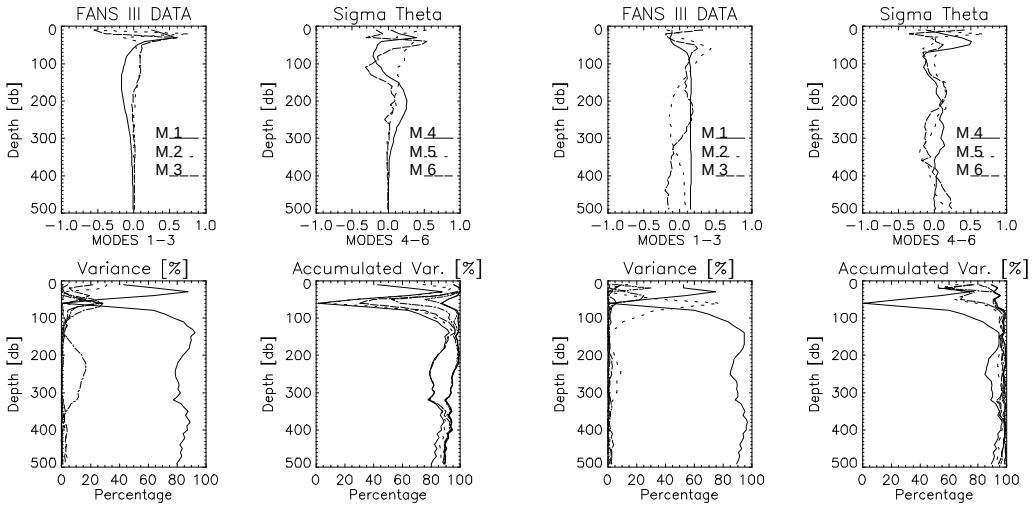

Figure 6-36 FANS III Sigma theta vector modes (6), explained variance and accumulated explained variance for the non-standardized (a) and standardized (b) analyses.

6.4.1.2 FANS II – Winter conditions

As mentioned previously, the average potential temperature profile range during the winter campaigns (FANS II and MEGO 94) is less tan one degree. And again the variance explained by the first modes is very wavy due to the zero crossing of the corresponding vectors both in the non-standardized and the standardized analyses, as it can be seen in Figure 6-37.

The differences between both analyses are not as important as in FANS III. On the one hand, the non-standardized analysis (frame (a)) manages to better fit the bottom layer (a 75% minimum versus 20% of FANS III), although it behaves rather poorly around 100 m (60%). The standardized analysis (frame (b)), on the other hand, improves with depth, with the lowest explained variance in the upper 10 m (55%). Again, the standardized model provides a better fit in an overall sense.

For the salinity field (Figure 6-38), the non-standardized model (frame (a)) fails to fit the bottom layer, as in the case of FANS III. Instead, the fraction of explained variance is very high (values over 90%) in the upper 350 m, i.e., even better than for the standardized case (frame (b)). Nevertheless, the latter is still better in an overall sense, since it manages to resolve the bottom layer.

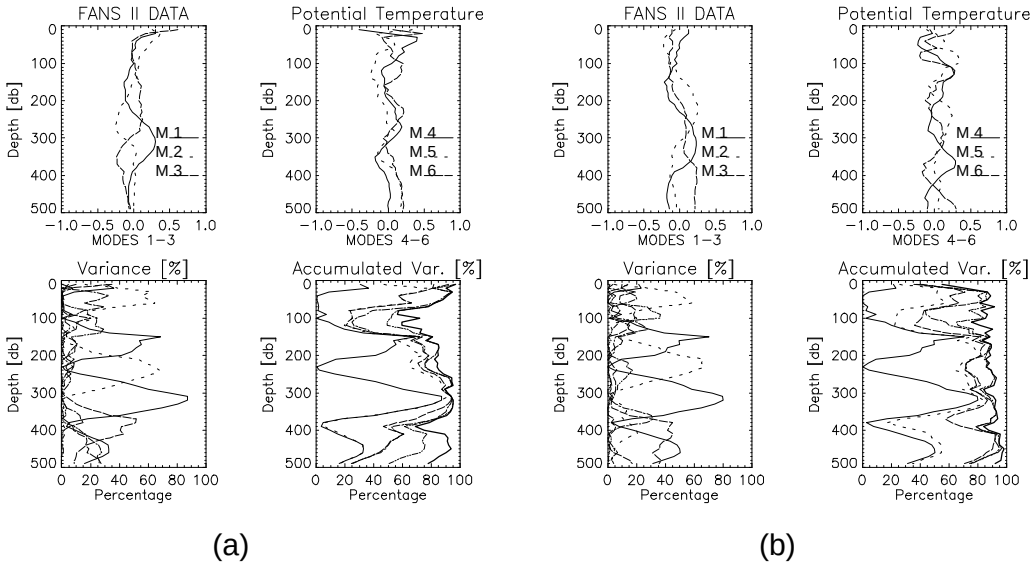

Figure 6-37 FANS II Potential temperature vector modes (6), explained variance and accumulated explained variance for the non-standardized (a) and standardized (b) analyses.

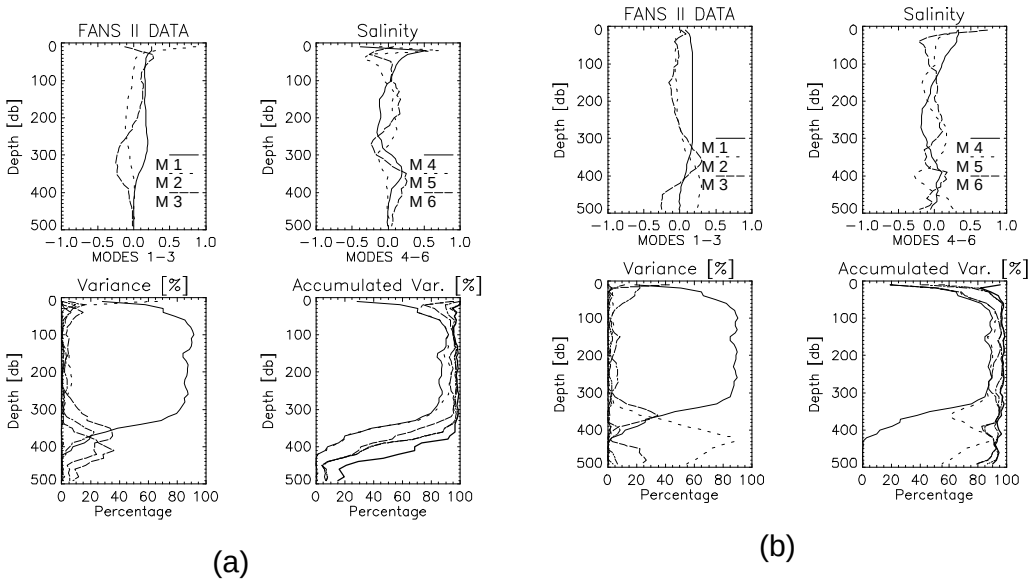

Figure 6-38 FANS II Salinity vector modes (6), explained variance and accumulated explained variance for the non-standardized (a) and standardized (b) analyses.

Since temperature plays a minor role in the winter overall density variations due to its small range of variability, it is not surprising that density results (Figure 6-39) resemble the salinity ones. Perhaps with the difference that with the non-standardized model the bottom layer is better explained than it was for previous variables.

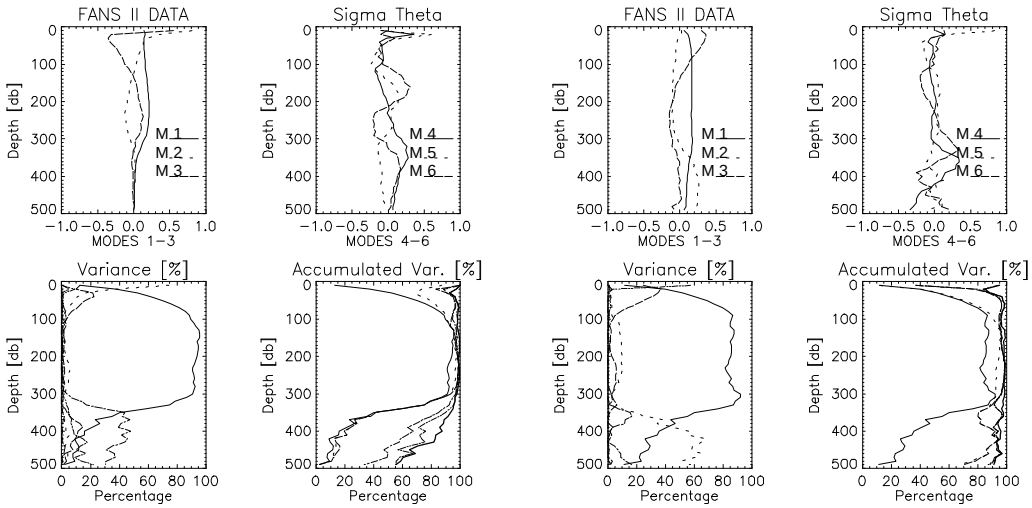

Figure 6-39 FANS II Sigma theta vector modes (6), explained variance and accumulated explained variance for the non-standardized (a) and standardized (b) analyses.

6.4.1.3 Some remarks on FANS I and MEGO 94.

For the remaining campaigns, FANS I and MEGO 94, the plots shown will limit to density. FANS I took place in autumn, therefore in a transition period between summer and winter conditions. Instead, MEGO 94 took place in winter, when mesoscale activity is reported to be intense. However, as it has been mentioned previously, the meteorological and sea conditions during this campaign were very calm and the spatial fields observed were rather homogeneous.

For the FANS I data set (Figure 6-40), the variance explained by the leading modes of the non-standardized model is in general low below 100 m, and very high above that depth (for the salinity field, the explained variance is low down to 170 m). Instead, the standardized analysis produces high

percentages of explained variance over the whole water column (except in the case of salinity, for which it is low in the upper 100 m).

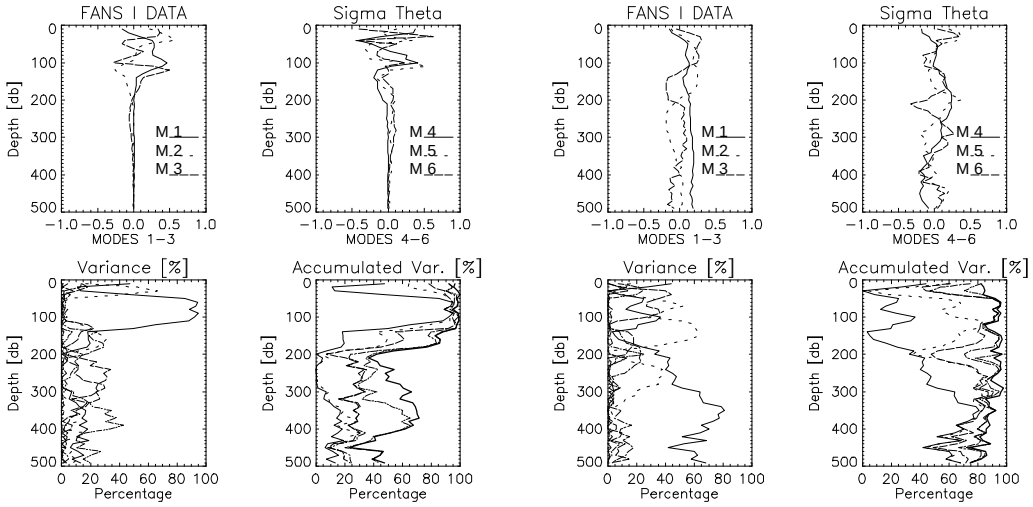

Figure 6-40 FANS I Sigma theta vector modes (6), explained variance and accumulated explained variance for the non-standardized (a) and standardized (b) analyses.

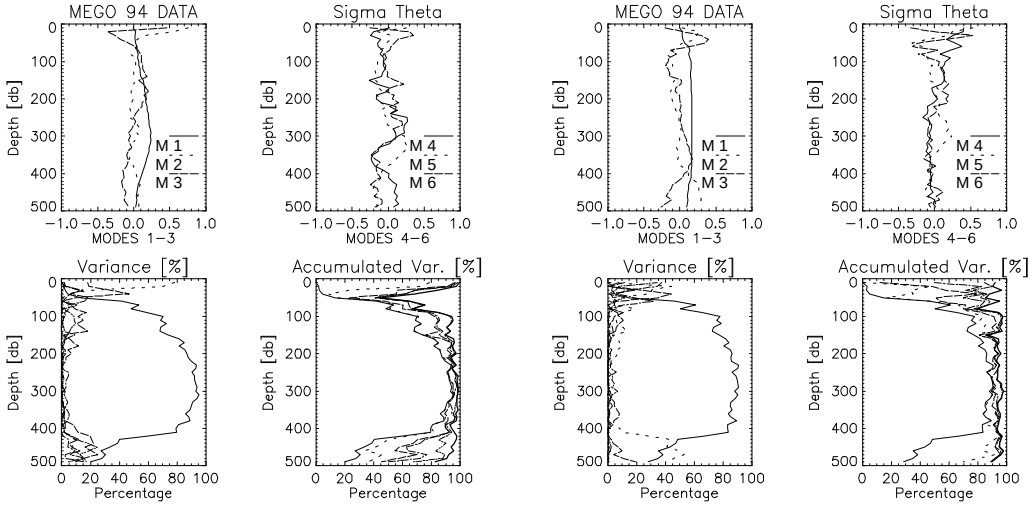

Figure 6-41 MEGO 94 Sigma theta vector modes (6), explained variance and accumulated explained variance for the non-standardized (a) and standardized (b) analyses.

For the MEGO 94 data set (Figure 6-41), the most notorious result is the similarity of the variance explained by the six leading modes of both type of

models. In fact, the first mode has a similar shape for both models and for all the variables, characterized by no zero crossings. The largest differences are found for density (shown below), and not in the bottom layer, as for all the other campaigns, but between 20 and 100 m.

6.4.1.4 Preliminary Conclusions

At this point, it could be stated that the standardized analysis produces better results, in the sense that the fraction of variance explained by the leading modes is apparently higher and more evenly explained over the water column. However, two key comments must be added to this statement.

The first one is that the reported plots show the percentage of variance explained at each level, regardless to the variance accounted by the level. In terms of total variance, the values obtained for each one of the variables, both with the non-standardized and standardized analyses, are shown in Tables 6-1 to 6-4. We present both the total variance percent and the accumulated variance as successive modes are considered. In general terms there are not significant differences between the non-standardized and the standardized analysis, with the exception of potential temperature in FANS III and FANS I. Nonetheless, the non-standardized analysis performs slightly better in all cases.

The second comment is that this preliminary conclusion is mainly valid for the stratified season, when the variance of the upper layers is significantly larger than the variance of lower layers. For the homogeneous season, the differences between both methods are not as significant, since the variance is more evenly distributed in the vertical.

	Mode	1	2	3	4	5	6
Potential Temperature	Non St.	74.1 74.1	13.7 87.8	7.0 94.8	2.1 96.9	1.3 98.1	0.5 98.6
	Stand.	48.3 48.3	13.8 62.1	10.1 72.2	7.5 79.7	4.8 84.4	3.4 87.8
Salinity	Non St.	67.9 67.9	12.5 80.5	9.1 89.6	4.3 93.9	1.9 95.8	1.0 96.7
	Stand.	72.4 72.4	8.9 81.3	6.9 88.2	3.5 91.7	1.7 93.4	1.7 95.1
Density	Non St.	75.1 75.1	10.7 85.7	7.2 92.9	4.0 96.9	1.6 98.5	0.6 99.1
	Stand.	82.8 82.8	8.5 91.3	2.1 93.4	2.0 95.4	1.3 96.7	1.0 97.7

Table 6-1 FANS III – Percentage of total explained variance (upper row on the cell) and accumulated explained variance (lower row) with the first six modes, for potential temperature, salinity and density.

	Mode	1	2	3	4	5	6
Potential temperature	Non St.	37.3 37.3	27.4 64.6	10.0 74.6	6.7 81.3	4.5 85.9	3.1 89.0
	Stand.	31.6 31.6	22.8 54.4	16.5 70.9	7.6 78.4	6.0 84.4	3.9 88.3
Salinity	Non St.	71.2 71.2	13.6 84.8	5.7 90.5	4.4 94.9	1.5 96.5	1.1 97.6
	Stand.	60.3 60.3	19.8 80.0	7.7 87.7	4.1 91.8	2.2 94.0	1.6 95.6
Density	Non St.	75.6 75.6	13.8 89.4	4.9 94.3	2.0 96.4	1.2 97.6	0.8 98.4
	Stand.	65.3 65.3	19.6 84.9	5.7 90.6	2.9 93.5	1.7 95.2	1.2 96.3

Table 6-2 FANS II – Percentage of total explained variance variance (upper row on the cell) and accumulated explained variance (lower row) with the first six modes, for potential temperature, salinity and density.

	Mode	**1**	**2**	**3**	**4**	**5**	**6**
Potential temperature	Non St.	78.5 78.5	11.6 90.2	3.4 93.5	2.4 96.0	1.7 97.6	0.7 98.4
	Stand.	45.7 45.7	15.7 61.4	8.9 70.3	8.0 78.3	5.6 83.8	3.2 87.1
Salinity	Non St.	47.8 47.8	17.1 64.9	11.3 76.2	4.5 80.7	3.9 84.6	3.1 87.7
	Stand.	41.9 41.9	17.1 59.0	11.8 70.8	7.0 77.8	4.7 82.5	3.0 85.4
Density	Non St.	73.8 73.8	12.8 86.5	4.7 91.3	3.7 94.9	1.6 96.5	1.0 97.5
	Stand.	43.3 43.3	21.2 64.6	10.3 74.9	8.5 83.3	3.8 87.1	2.5 89.6

Table 6-3 FANS I – Percentage of total explained variance variance (upper row on the cell) and accumulated explained variance (lower row) with the first six modes, for potential temperature, salinity and density.

	Mode	1	2	3	4	5	6
Pot. Temp	Non St.	60.8 60.8	16.8 77.6	6.4 84.0	4.8 88.9	3.0 91.8	2.2 94.0
	Stand.	51.4 51.4	18.4 69.7	11.2 80.9	5.3 86.2	3.3 89.5	2.5 92.0
Salinity	Non St.	70.6 70.6	14.8 85.4	4.8 90.2	3.6 93.8	1.5 95.3	1.1 96.5
	Stand.	61.2 61.2	14.9 76.1	9.3 85.4	5.8 91.2	2.0 93.3	1.6 94.9
Density	Non St.	75.4 75.4	9.1 84.5	5.6 90.1	2.4 92.4	2.1 94.6	1.4 95.9
	Stand.	67.2 67.2	12.4 79.6	5.7 85.3	4.6 89.9	2.5 92.4	1.4 93.8

Table 6-4 MEGO 94 – Percentage of total explained variance variance (upper row on the cell) and accumulated explained variance (lower row) with the first six modes, for potential temperature, salinity and density.

And, in any case, the convenience of one method or another will depend on the ultimate objectives of the analysis, e.g., on whether the variability of upper layers is considered more important or, instead, the structure of the whole water column is to be reproduced.

6.4.2 The Representativity test

When a cast is shallower than the depth of the EOFs, the principal components of the profile can no longer be computed simply as the scalar product between the profile and each of the EOFs. In such case there are different methods to estimate the components (e.g., by a simultaneous least square fit). Here we will follow the method proposed by Haney et al (1995) (refer to Chapter 3), which consists of estimating the amplitudes in a sequential way. The aim is to include as much as possible of the field variance in the first modes.

In the campaigns of our interest many of the casts do not reach the required depth (the percentage of deep casts ranges between 13% and 25%, (refer to Table 5-1). Furthermore, the dynamics of the region can have significant local signals, both through the Ebro River outflow and through meteorological conditions. Therefore, finding out the extent to which shallow profiles (those reflecting mainly the shelf dynamics) can be expressed in terms of the leading EOFs (which usually reflect the shelf break and offshore dynamics) constitutes an interesting test.

The results of this test will be quantified in terms of error profiles, which will show the remaining fraction of unexplained variance after including additional components to the fit. If they were calculated with the deep casts only, these error curves would be complementary to the accumulated variance percentage Figures of the previous section (i.e., the sum of the two curves corresponding to the same number of modes would be equal to 100 at every level).

In the following Figures this will not be at all the case. In fact, there is no reason for some (apparently) peculiar results to be obtained, namely:

Error percentages higher than 100%.

An increase in the error percentage after adding an additional mode

Obviously, none of the above results could have been obtained when considering the deep casts only.

For a given number of EOFs *M*, the errors fraction at a level *j* is estimated by the following expression:

$$Err_j = \left[\frac{\sum_{i=1}^{N} \left(D_i - \hat{D}_i\right)^2}{\sum_{i=1}^{N} \left(D_i - < D >\right)^2} \right] * 100 \qquad \textbf{(6-1)}$$

where D_i stands for the value (at level *j*) of the *i-th* cast (or station), $\hat{D}_i$ stands for the corresponding value estimated using *M* EOFs, and $< D >$ is the *j-th* level mean value (averaged over the *N* casts available at that level). The plots with the number of casts available at each depth *N(j)* have already been plotted in Chapter 5 for each of the campaigns,.

In the following sections we will also show contour Figures with three plots. The upper two will correspond to the fields obtained from (the six leading modes of) the non-standardized (left) and standardized (right) analyses. The bottom plot corresponds to the contouring of the data themselves. Contour Figures corresponding to two depth levels are shown, usually 10 and 100 m. Finally, as in the data chapter, we also show transversal section contour plots corresponding to four transects, again as they result from the EOFs fit following the two analysis models. All the Figures have been obtained by interpolating station data onto grid point data using the reported SC procedure.

6.4.2.1 FANS III

The potential temperature error profiles (Figure 6-42) reach values higher than 100% at particular levels even using four modes of the non-standardized analysis, while it only does the same using the single first mode of the standardized method. In fact, the addition of the second and third modes in the non-standardized case does not significantly improve the fit. Nonetheless, while the error in the upper 30 m in the first case is zero, in the second it is nearly 50%. In order to get a proper idea about what these errors represent, we will show horizontal contour plots at different levels.

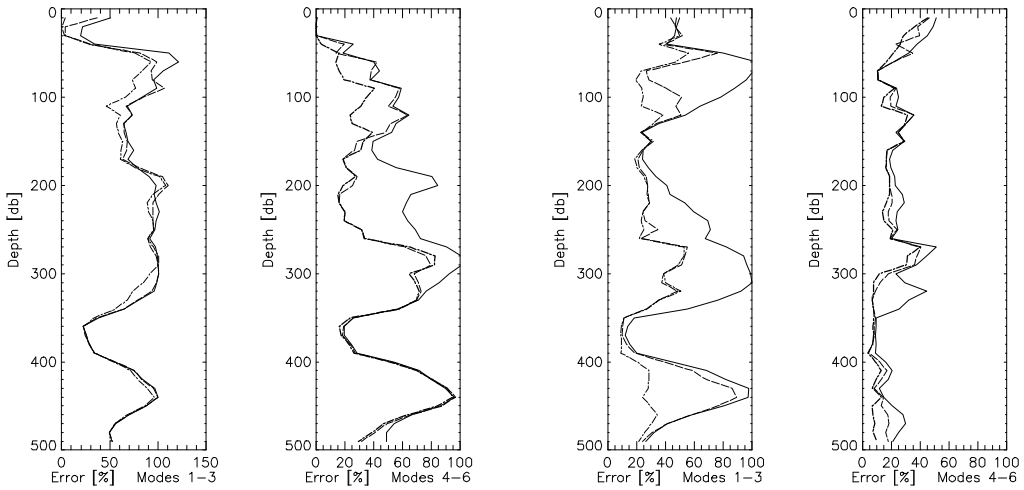

Figure 6-42 FANS III Potential temperature error profiles, considering six successive modes, for the non-standardized (a) and standardized (b) analyses.

In this and similar Figures, successive lines correspond to the error considering an additional mode. The full line corresponds to modes 1 and 4, the dashed line to modes 2 and 5, and dash-dot line to modes 3 and 6. The thick line corresponds to the error profiles with the first six modes.

At 10 m (Figure 6-43) the non-standardized analysis is rather closer to actual data, the largest differences being to the south of the Ebro Delta. Instead, there are more notorious differences between actual data and the standardized analysis. In this case, the overall structure is well represented, but with a larger range to the southern sector of the domain adjacent to the coast. At this depth, the mean error of the standardized analysis (always considering the six leading modes) is around 45%, while it is nearly zero for the non-standardized analysis.

The previous situation changes significantly at 300 m, where the error with the non-standardized case is higher than 70%, while it is around 15% for the standardized one. Figure 6-44 shows the distributions for both cases, revealing that the overall structure has been lost in the non-standardized case. The standardized model resembles more the data, though with some more pronounced structures.

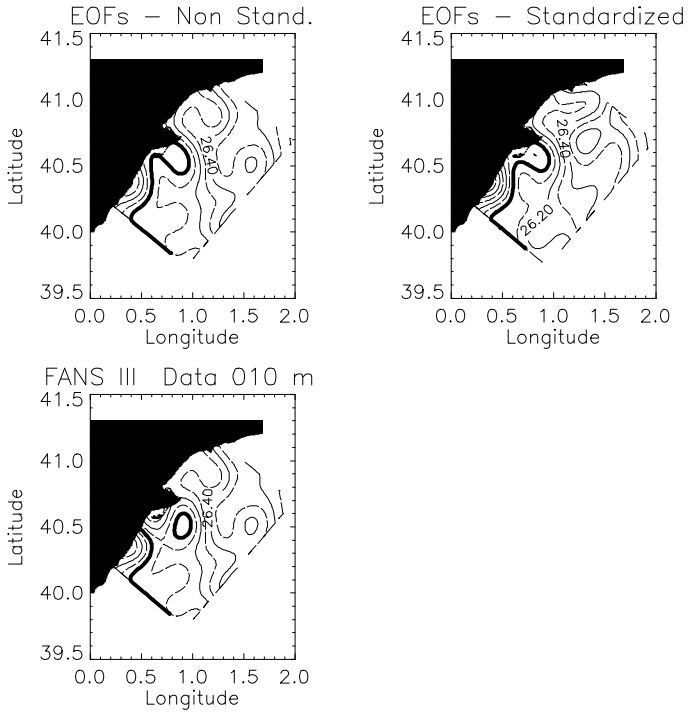

Figure 6-43 FANS III Potential temperature contour lines at 10 m. Successive contours differ in 0.5°C and the thick line marks the 22°C isotherm.

In this and all similar Figures the upper left frame shows the results with the first six modes in the non-standardized analysis, the upper right shows the equivalent results with the standardized one, while the data is shown in the bottom frame. These plots have been done with gridded data after the SC interpolation.

The salinity error profiles present the two odd characteristics mentioned above: errors are locally higher than 100% and adding subsequent modes results in local error increments (Figure 6-45, frame a). Namely, the addition of the fourth mode increases the error at 30 m up to a 170%, decreasing afterwards when higher modes are added. Since most of the variability is in the upper 100 m, the addition of successive modes does not significantly improve the fit below 300 m. Nevertheless, since in shallow regions principal components are estimated successively, the error in the 10 – 20 m layer is zero.

On the other hand, the standardized analysis (frame b) produces error profiles that do not differ significantly in shape compared to those obtained for the deep casts only, though the values are slightly higher, specially in the upper 100 m. The error at 10 m is nearly zero, increasing up to 40% (the highest value) at 30 m.

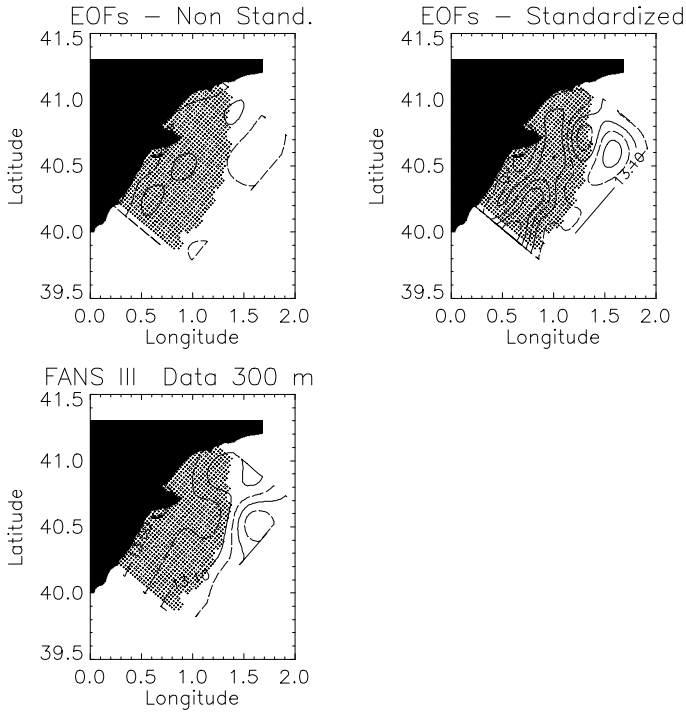

Figure 6-44 FANS III Potential temperature contour lines at 300 m. Successive contours differ in 0.05°C.

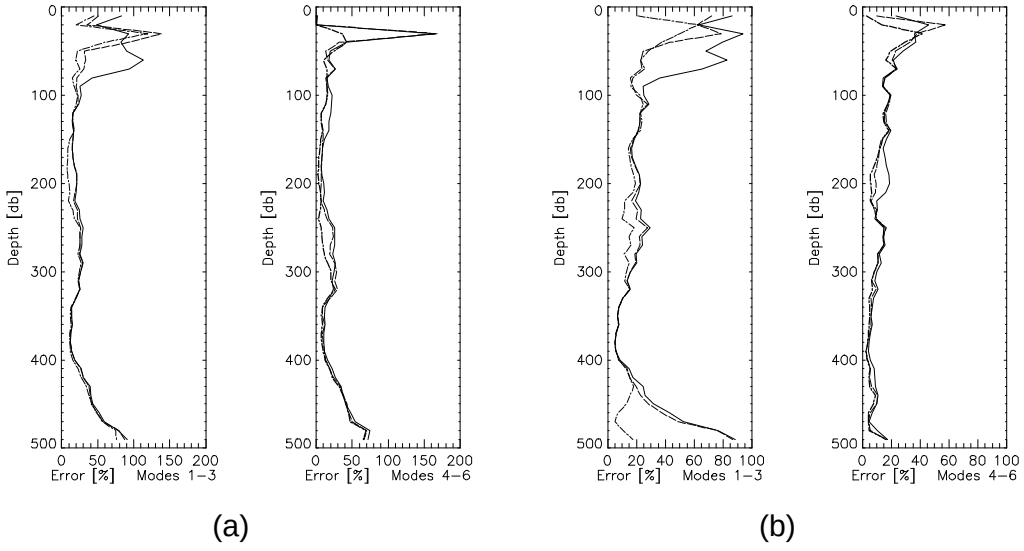

Figure 6-45 FANS III Salinity error profiles, considering six successive modes, for the non-standardized (a) and standardized (b) analyses.

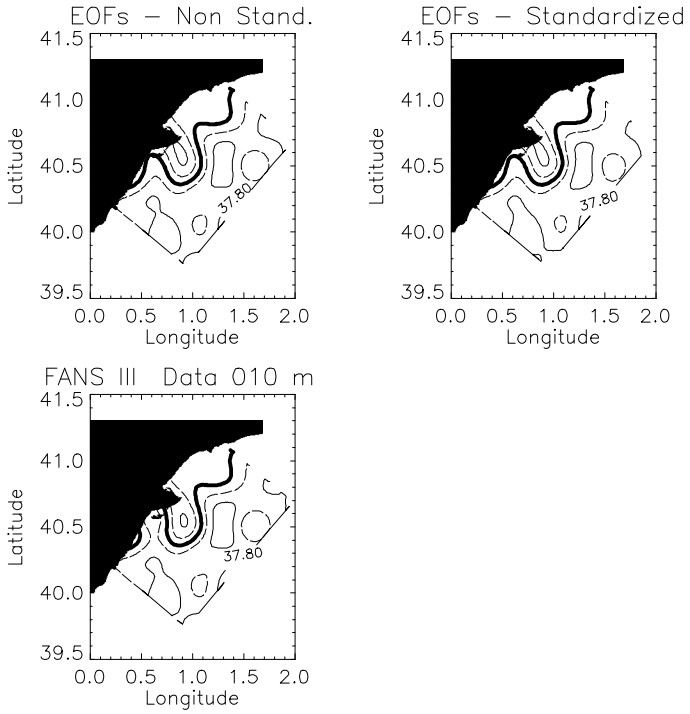

Figure 6-46 FANS III Salinity contour lines at 10 m. Successive contours differ in 0.1 and the thick line marks the 37.4 isohaline.

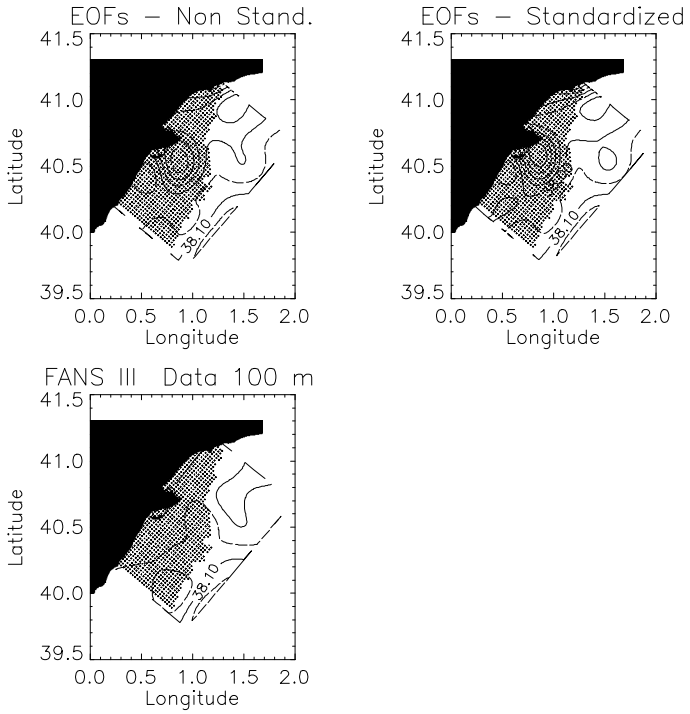

Figure 6-47 FANS III Salinity contour lines at 100 m. Successive contours differ in 0.05

Since the error with both models is nearly zero, the salinity distribution at 10 m is practically identical to the data (Figure 6-46). At 100 m is, errors are close to 20% for both cases, and the salinity distributions of the two models do not differ significantly (Figure 6-47). The differences with respect to actual data are more notorious in the northern half of the study area, but they are not specially large, and again the structure is well represented.

The density error profiles (Figure 6-48) for the non-standardized case (frame a) show the best overall fit of the three variables. This fact will be important for the estimate of geostrophic currents. The lowest error is found in the upper 30 m, while the largest (around 45%) is found at 60 m. Nonetheless, the error profile with the standardized analysis is definitely better in an overall sense, except in the upper 40 m, where the error is higher than for the non-standardized case.

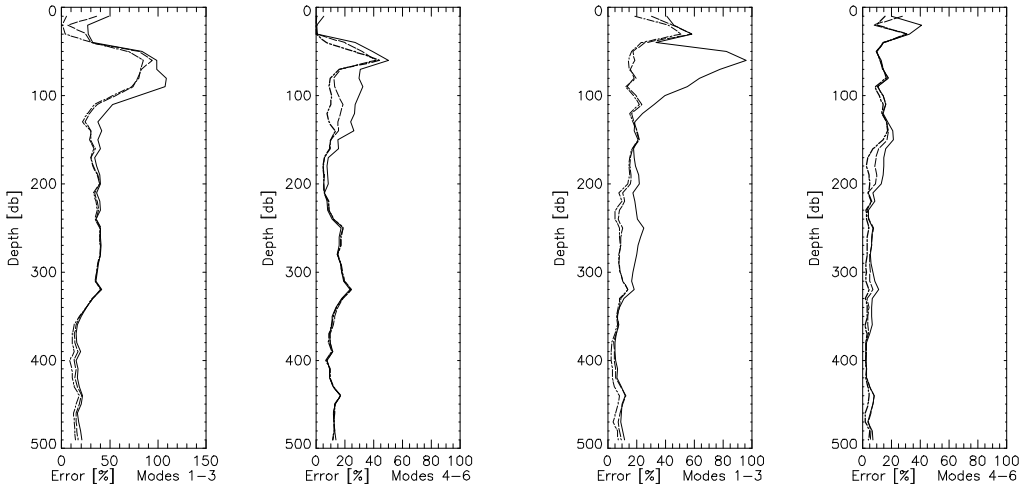

Figure 6-48 FANS III Density (sigma theta) error profiles, considering six successive modes, for the non-standardized (a) and standardized (b) analyses.

These results reflect in the horizontal distributions: at 10 m (Figure 6-49) there are no significant differences between the data and the non-standardized contour lines, while some differences are observed in the standardized analysis.

In the latter, there is a more pronounced structure in the southern part of the domain, adjacent to the coast, similar to the temperature case, and a slightly different distribution is also found in the northern half of the domain.

At 100 m we find error values of around 10% in both cases, and the distributions (Figure 6-50) of both analyses are very similar. In the north-eastern region they differ from the data, producing slightly more pronounced structures, though the general distribution is well represented.

In order to get a more complete view of the differences between both models and between them and actual data, we also present transversal section plots for the four transects presented in the “Data” chapter. We will only show the density distributions obtained from the non-standardized (Figure 6-51) and the standardized (Figure 6-52) analyses.

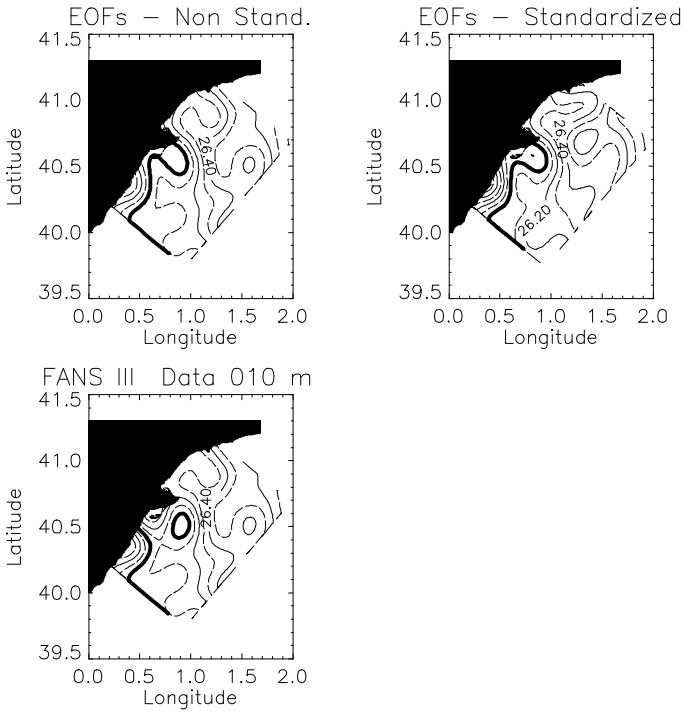

Figure 6-49 FANS III Density contour lines at 10 m. Successive contours differ in 0.1, the thick line marks the 26 isopycnal.

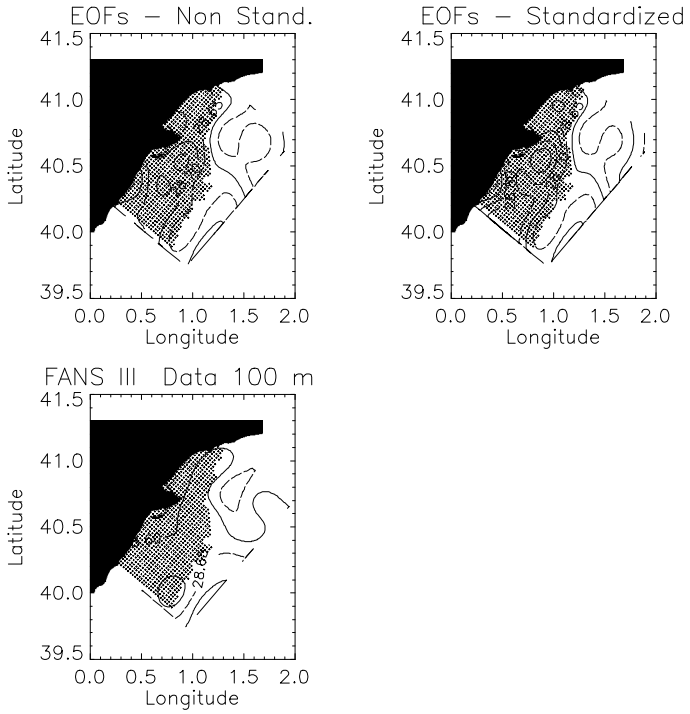

Figure 6-50 FANS III Density contour lines at 100 m. Successive contours differ in 0.05.

The distributions of both models are nearly identical, perhaps the most notorious difference is the downward tilting of the 28.5 isopycnal (underneath the thick line) towards the seaward edge in the standardized case, in transects A and B. Comparing both Figures with their data equivalent (Figure 6-26), it is clear that the analyses reproduce very well the overall distribution, though some differences are observed underneath the pycnocline. Again, the most notorious difference is in the 28.5 isopycnal in the standardized case, transect A, where there is a difference in depth with the data of nearly 40 m at the seaward edge.

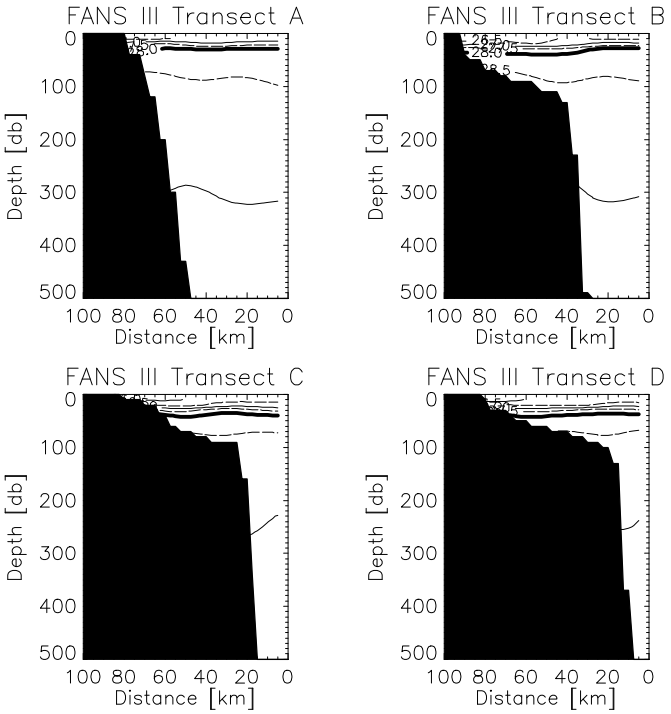

Figure 6-51 Density transects for FANS III for the non-standardized analysis. The 28 isopycnal has been marked by a thick line. Successive isolines have a 0.5 difference.

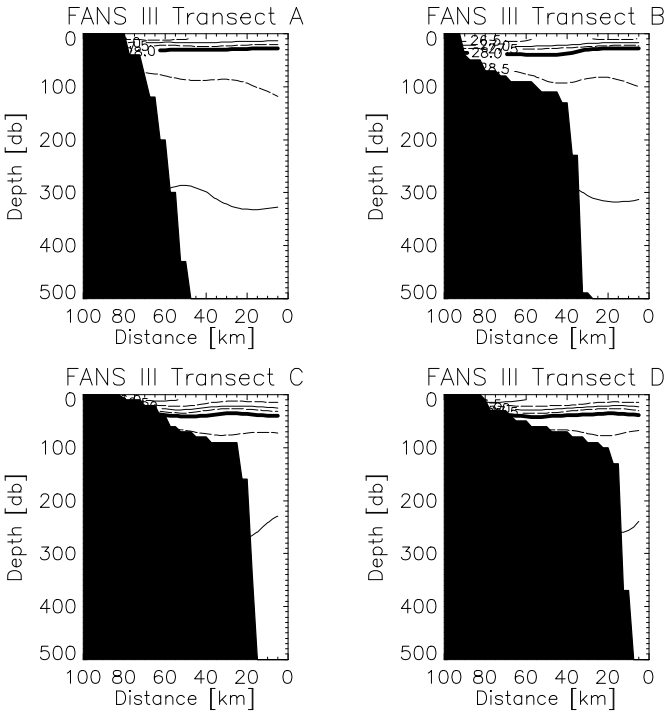

Figure 6-52 Density transects for FANS III for the standardized analysis.

6.4.2.2 FANS II

The error profiles of potential temperature (Figure 6-53) show an overall fit, with six modes, that proves to be better with the standardized analysis, though the non-standardized one has lower errors in the first 30 m. This reflects in Figure 6-54, where the contour distribution of the non-standardized case is closer to the data distribution, though the standardized results are not too different either.

At 100 m (Figure 6-55) the standardized analysis provides a better fit in a statistical sense and therefore follows more closely the contour distribution of the data than the non-standardized one. Nevertheless, both models reproduce well the eddy structure at the northern boundary, as well as the rather homogeneous sea-ward region.

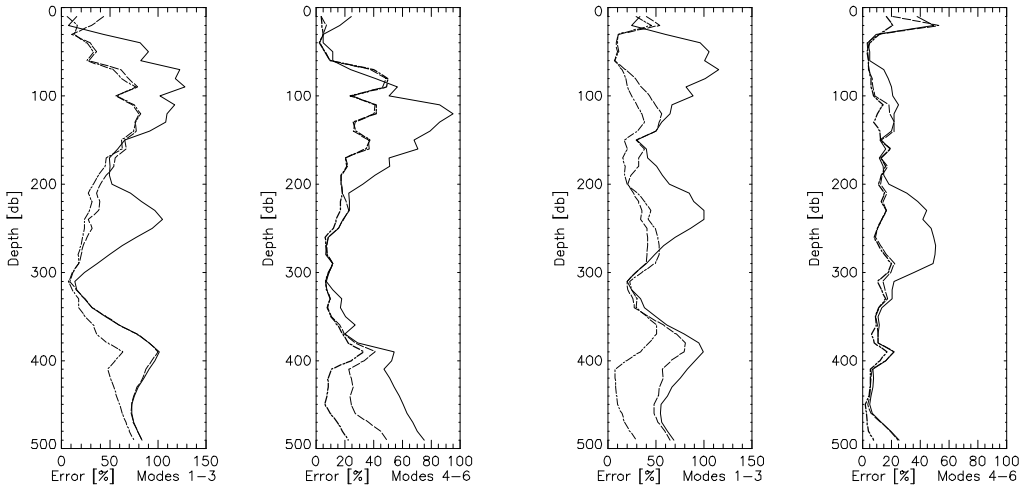

Figure 6-53 FANS II Potential temperature error profiles, considering six successive modes, for the non-standardized (a) and standardized (b) analyses.

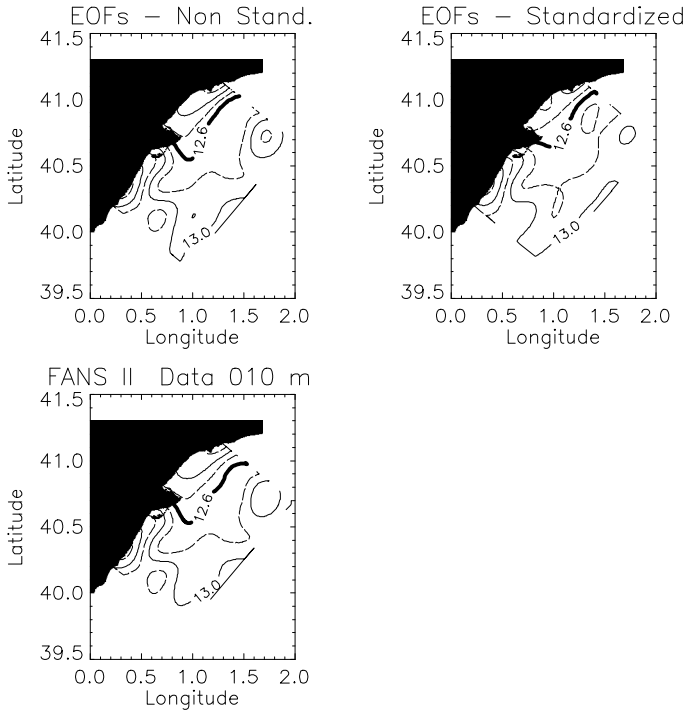

Figure 6-54 FANS II Potential temperature contour lines at 10 m. Successive contours differ in 0.2°C and the thick line marks the 12.6°C isotherm.

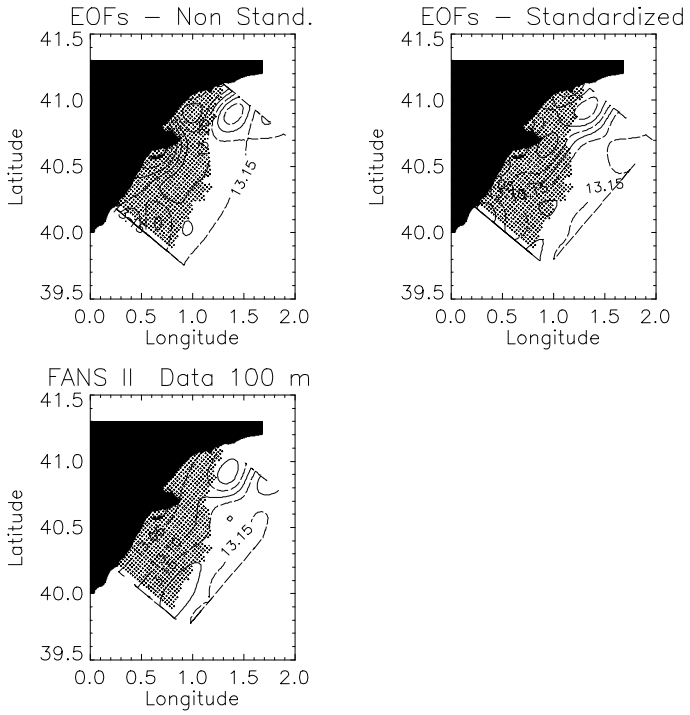

Figure 6-55 FANS II Potential temperature contour lines at 100 m. Successive contours differ in 0.05°C.

In the case of salinity, the error profiles with six modes are very similar in the first 380 m (Figure 6-56) for both analyses, but beneath that depth the non-standardized model fails to reproduce the data (errors as large as 95%). Instead, the standardized analysis errors remain lower than 15% at all depths. In fact, the error decreases in the upper 40 m when adding additional modes, while in all the previous cases it either increases or remains nearly equal.

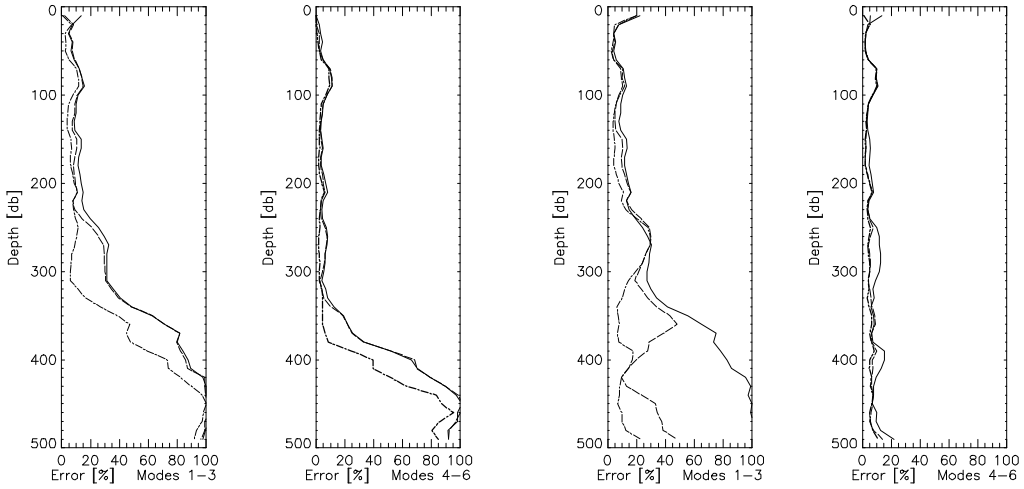

Figure 6-56 FANS II Salinity error profiles, considering six successive modes, for the non-standardized (a) and standardized (b) analyses.

Since the error is practically zero at 10 m, the salinity distribution of the non-standardized analysis is identical to the data (Figure 6-57, frame a). For the standardized analysis the contour lines differ slightly, but reproduce the overall pattern.

At 100 m (Figure 6-58) the salinity distribution obtained with both analyses is practically identical. Compared to the data, both models slightly smooth the wavy structure and miss an eddy-like structure near the northern boundary, which is clearly depicted in potential temperature. Apart from these differences, results are acceptable.

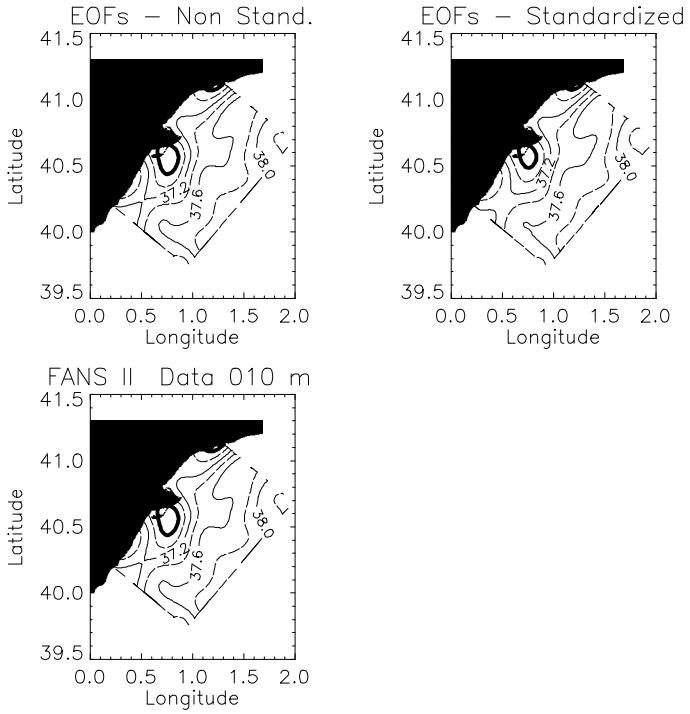

Figure 6-57 FANS II Salinity contour lines at 10 m. Successive contours differ in 0.2 and the thick line marks the 36.8°C isohaline.

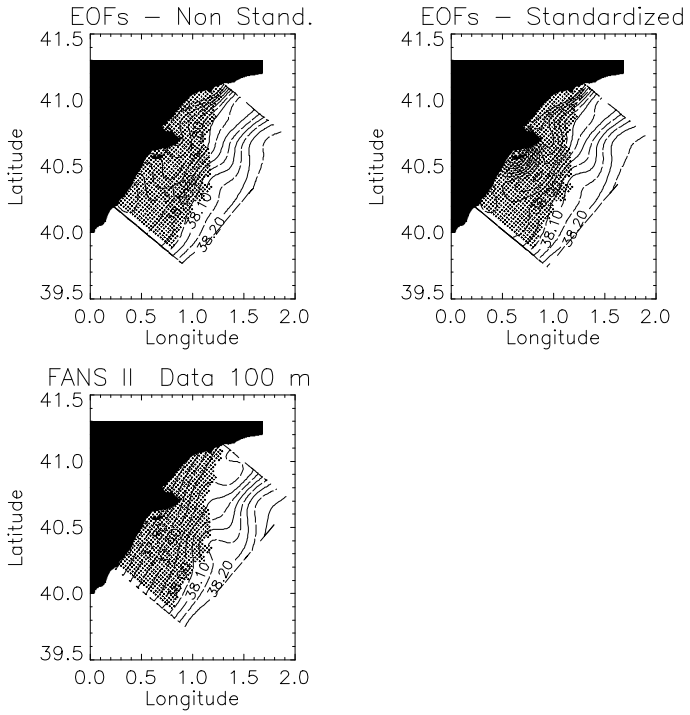

Figure 6-58 FANS II Salinity contour lines at 100 m. Successive contours differ in 0.05.

For the density field, comments are similar to those made for salinity, both for the error profiles (Figure 6-59), and for the contour distributions at 10 (Figure 6-60) and 100 m (Figure 6-61). This is not surprising, since the temperature range in this campaign, as well as in MEGO 94, is very low, and therefore its contribution to density variability is very low.

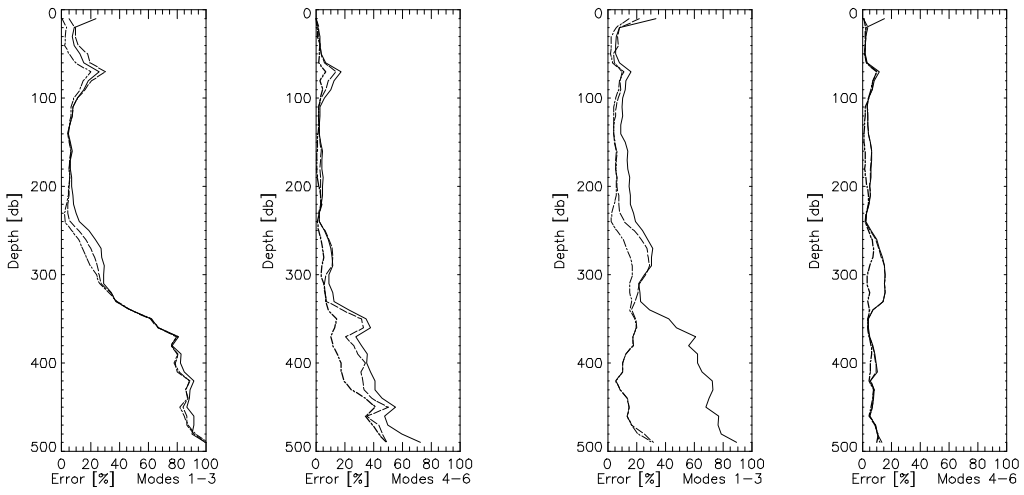

Figure 6-59 FANS II Density error profiles, considering six successive modes, for the non-standardized (a) and standardized (b) analyses.

The contour distribution at both depths is closer to the data for the non-standardized analysis, but the standardized results are also very similar. Still, the error profiles show very clearly the fact that the standardized model gives better results when at depths greater than 300 m, whereas non-standardized model errors increase from around 10% at that depth to nearly 50% at 490 m.

To understand the significance of these large errors at depths where the variance is so small it is worth recalling that reported errors are weighted by the variance of the corresponding depth. This means that at a depth with variability approaching zero, the error would approach infinite, regardless of the ability of a given model to approach the data.

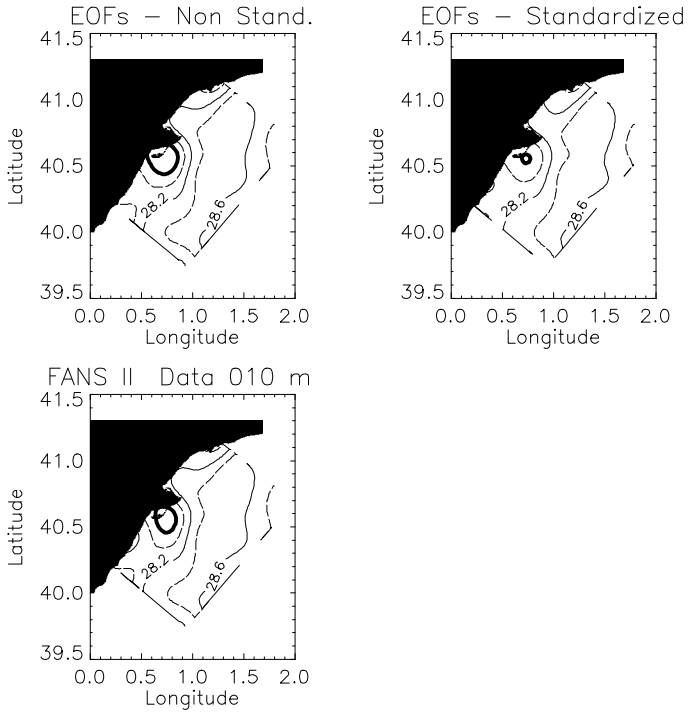

Figure 6-60 FANS II Density contour lines at 10 m. Successive contours differ in 0.2 and the thick line marks the 27.8 isopycnal.

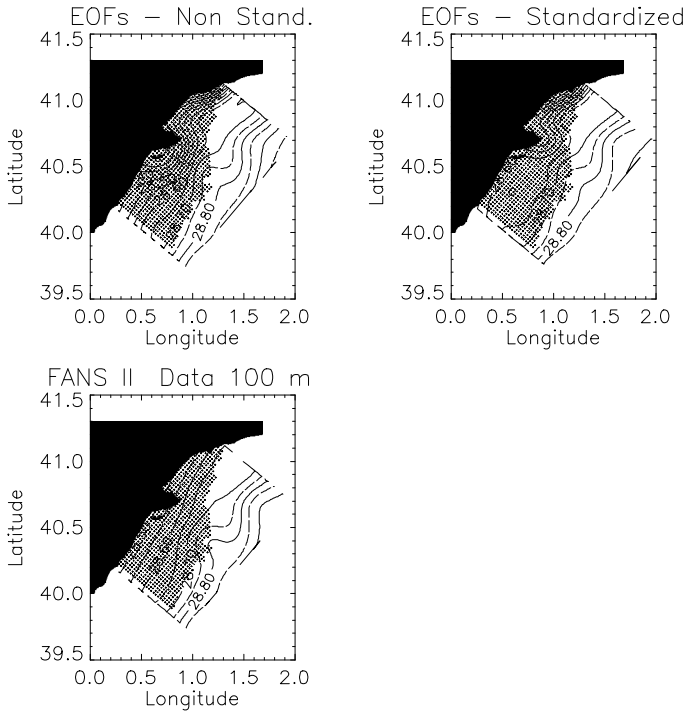

Figure 6-61 FANS II Density contour lines at 100 m. Successive contours differ in 0.05.

Transversal sections give a good idea of the vertical variability, and the results of both the non-standardized (Figure 6-62) and standardized (Figure 6-63) analyses can easily be compared with the data (Figure 6-22).

In general, the isopycnals resulting from the EOF analyses tend to be somehow smoother. Although the overall distribution is well represented by both models, there are some differences, particularly in transects A and B.

In the non-standardized analysis, in transect A, the 28.6 isopycnal (one above the thick line) tilts very strongly down to a depth of around 130 m, where it reaches the shore. The 28.8 isopycnal (thick line) follows very closely the data but its shape changes close to land at around 230 m. The 29 isopycnal is about 20 meters higher at the sea-ward boundary. The differences are less notorious in the other transects. Since the variability is very low below 350 m (refer to the standard deviation profile, the relatively large errors that result with this model do not seem to be important.

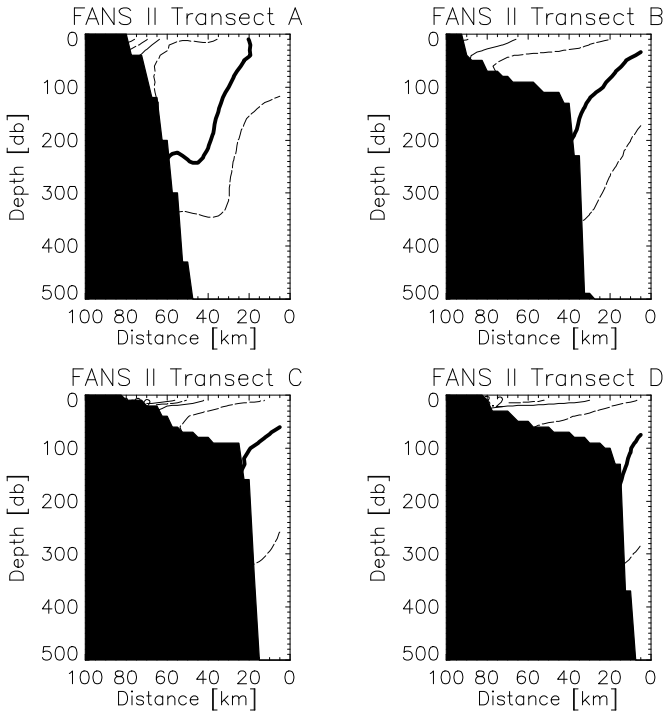

Figure 6-62 Density (sigma theta) transects for FANS II for the non-standardized analysis.

For the distribution produced by the standardized analysis the most significant difference with respect to actual data is also found in transect A. While the 28.6 isopycnal tilts downward (though less than in the previous analysis) the 29 isopycnal reaches the sea-ward boundary about 60 m lower than the data. There are also differences in the other transects, but they are not as notorious as in this one.

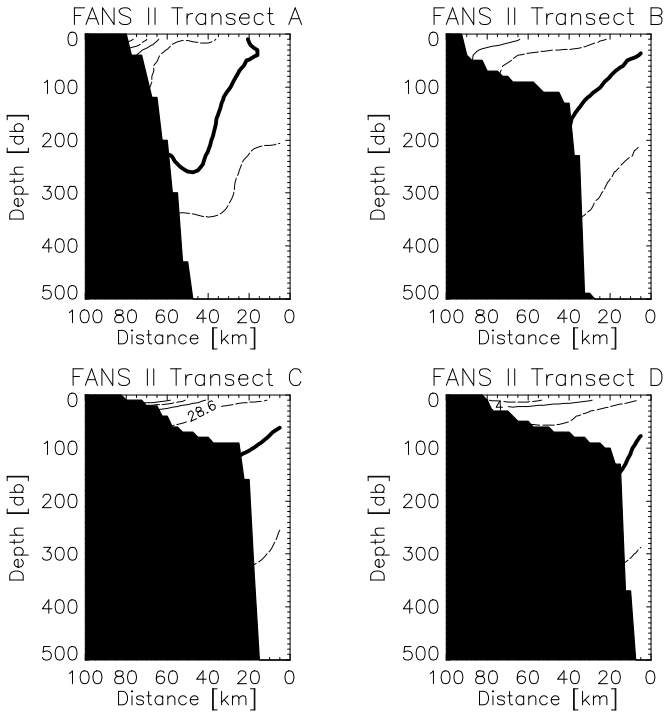

Figure 6-63 Density (sigma theta) transects for FANS II for the <u>standardized</u> analysis.

6.4.2.3 Some Remarks on FANS I and MEGO 94

As in the previous section, only density results will be reviewed for this two campaigns.

The errors of the non-standardized analysis (Figure 6-64, frame a), increase in the upper 100 m when considering all the casts, from less than 10% to more than 20% at the surface, and nearly that value between 60 and 80 m. From 140 m downwards the errors are quite high, from 40% to nearly 80%.

On the other hand, the errors with the standardized analysis (frame b) are higher in the upper 130 m and lower all the way down to the bottom.

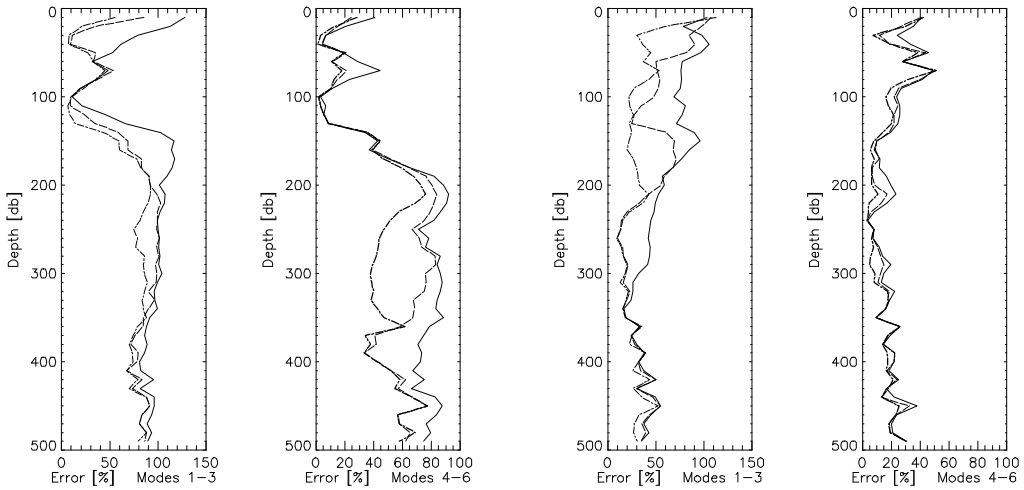

Figure 6-64 FANS I Density error profiles for the non-standardized (a) and standardized (b) analyses.

The contour lines that result from the non-standardized analysis at 10 m (Figure 6-65) have a closer resemblance to the data than the standardized ones (22% error vs 42%). The 27.1 isoline (thick line in all plots), which can be taken as an indicator of the Ebro River plume, differs in shape in the north-western area, while the eddy-like structure in the north-eastern side is well represented.

The standardized analysis results in a “plume” signal displaced to the south near the coast, and also extends over an area significantly larger than the data. The eddy structure is well depicted but has smaller gradients.

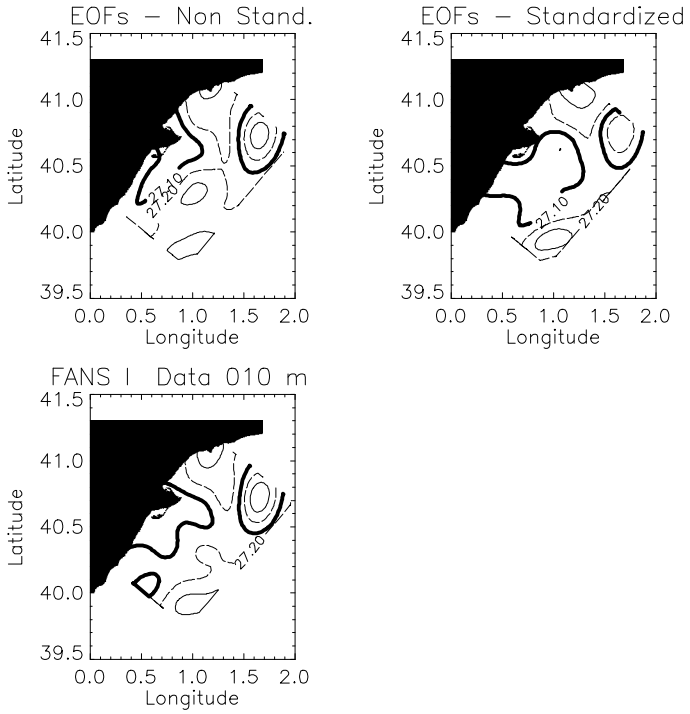

Figure 6-65 FANS I Density contour lines at 10 m. Successive contours differ in 0.1 and the thick line marks the 27.1 isopycnal.

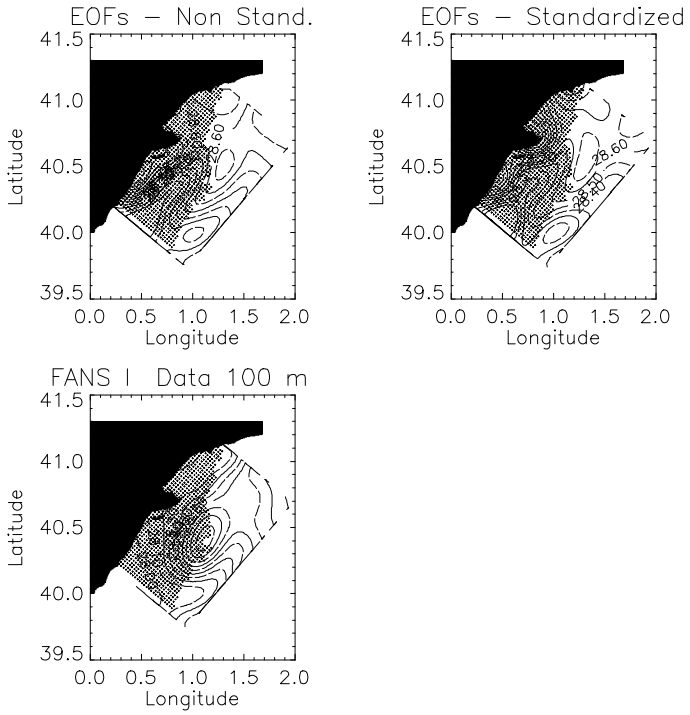

Figure 6-66 FANS I Density contour lines at 100 m. Successive contours differ in 0.1

The non-standardized analysis at 100 m (Figure 6-66, frame a) reproduces very closely the southern half of the study domain, with its wavy structure, though the isolines are more widely spread on the sea-ward boundary. This aspect is even more notorious in the standardized analysis (frame b). On the other hand, none of the models manages to reproduce well the northern third of the area.

As mentioned previously, the FANS I campaign was carried out during autumn, which implies a transition between summer and winter conditions. The presence of an eroded pycnocline is quite clear both on the actual data transversal sections (Figure 6-19) and on the equivalent Figures for the non-standardized (Figure 6-67) and the standardized (Figure 6-68) analyses.

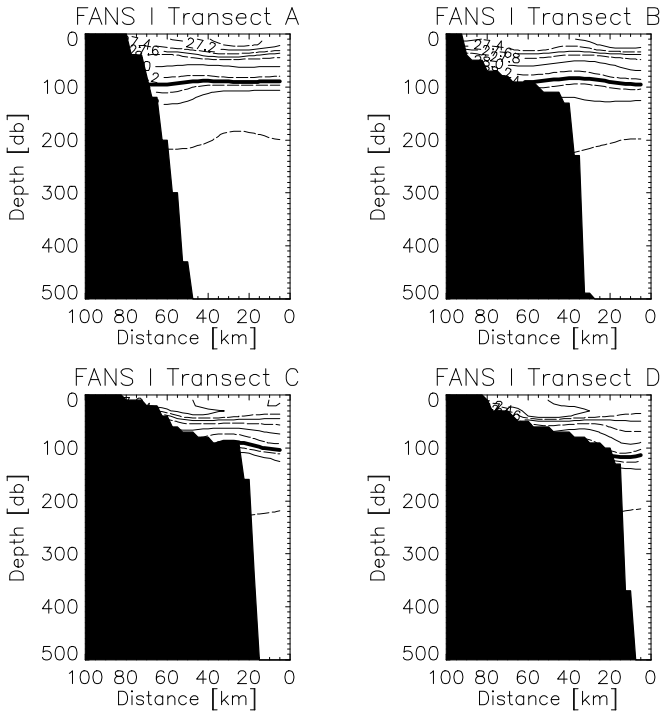

Figure 6-67 Density (sigma theta) transects for FANS I for the non-standardized analysis with the first six modes. The 28.4 isopycnal has been marked by a thick line. Successive isolines have a 0.2 difference.

There are some significant differences between the data and the model analysis, particularly at mid-depths. While the upper 60 m is well reproduced in transects A and B, below that depth the EOFs show a tendency to keep the isopycnals more horizontal, missing the bending towards land. This effect is

very evident with the 29 isoline in transects A and B (the lowest in all frames of all these Figures). The differences in transects B and C are less notorious, in fact, except the shape of the uppermost isopycnal, the other ones are similar. Very similar comments can be made for the standardized analysis.

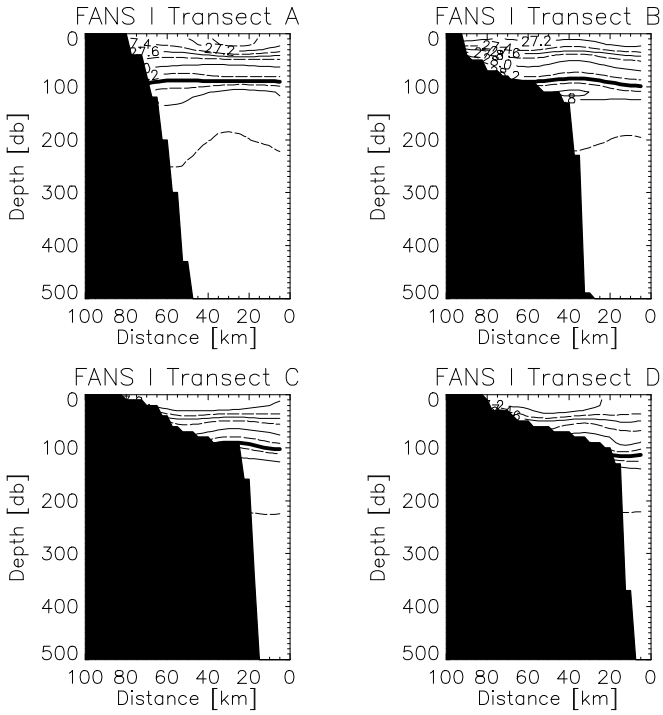

Figure 6-68 Density (sigma theta) transects for FANS I for the <u>standardized</u> analysis with the first six modes.

The error profiles corresponding to the six leading modes of the MEGO 94 campaign (Figure 6-69) reflect levels in which the EOF fitting procedure fails, producing errors as large as 200% at 60 m in the non-standardized analysis (frame a), and 100% at 20 m in the standardized one (frame b). In this latter case, the addition of the sixth mode worsens the error profile at this depth, duplicating it. Below 100 m, errors tend to be lower than 20% for both cases. If we refer to Figure 6-41 in order to compare the accumulated explained variance considering the deep casts only, the conflicting layer is also present in the non-standardized analysis, but with lower error values.

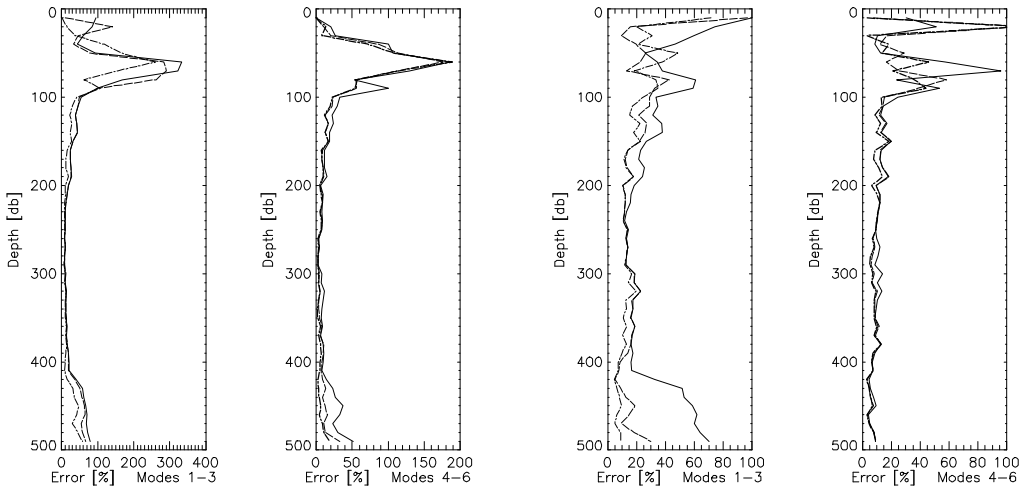

Figure 6-69 MEGO 94 Density error profiles, considering six successive modes, for the non-standardized (a) and standardized (b) analyses.

Another worth commenting aspect of the results of the non-standardized analysis is that the layers where the model fits fails are those with the lowest variability of the whole profile, both considering all the casts or the deep casts only.

While the error profiles have this conflicting layers, at 10 m the values are very low and this reflects in the density distributions (Figure 6-70). The non-standardized model results in a nearly identical distribution, while the standardized one approaches the data closely. Even though it has been mentioned in the data chapter, we wish to call the reader's attention to the fact that nearly all the structure is due to the Ebro Delta outflow, with nearly no variability in the northern third of the region.

Perhaps the most conspicuous aspect at 100 m (Figure 6-71). is the little structure observed. The error values are within the ranges observed for the other campaigns, less than 30% and around 15% for both models, but the layer is quite homogeneous, with a standard deviation of 0.008 considering all the available casts.

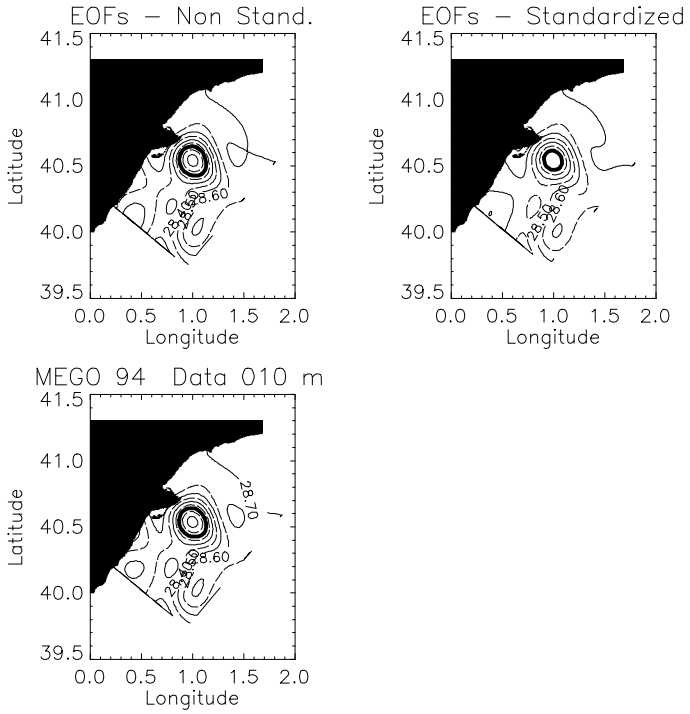

Figure 6-70 MEGO 94 Density contour lines at 10 m. Successive contours differ in 0.1 and the thick line corresponds to the 28.1 isopycnal.

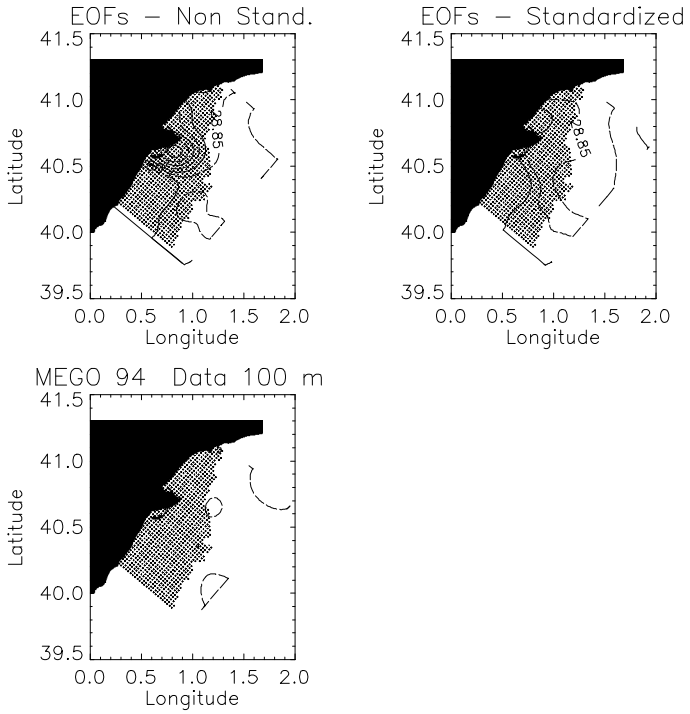

Figure 6-71 MEGO 94 Density contour lines at 100 m. Successive contours differ in 0.05.

The overall vertical view provided by the transversal section plots from the non-standardized (Figure 6-72) and standardized (Figure 6-73) models show a vertical density distribution that does not differ very significantly, at least apparently, from the data (Figure 6-29).

The most notorious difference with the first model is found in transect A, where the 29 isopycnal has a different shape and is 50 m higher at the sea-side than the data. The 28.8 is also slightly different. In transect C, the 28.8 isopycnal is also slightly deeper in the data. The largest difference that results with the standardized analysis is also in transect A, where the 29 isopycnal is 100 m higher at the sea-ward side of the domain.

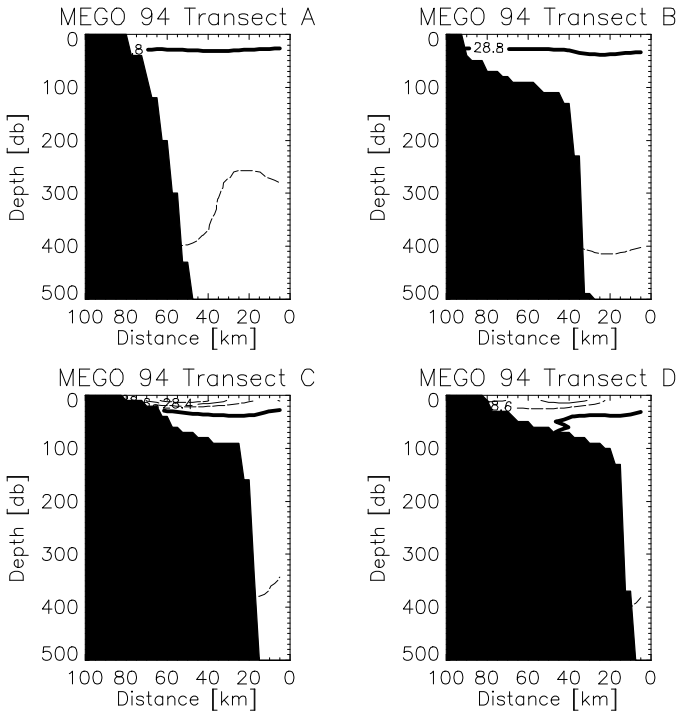

Figure 6-72 Density (sigma theta) transects for MEGO 94 for the <u>non-standardized</u> analysis with the first six modes. The 28.8 isopycnal has been marked by a thick line. Successive isolines have a 0.2 difference.

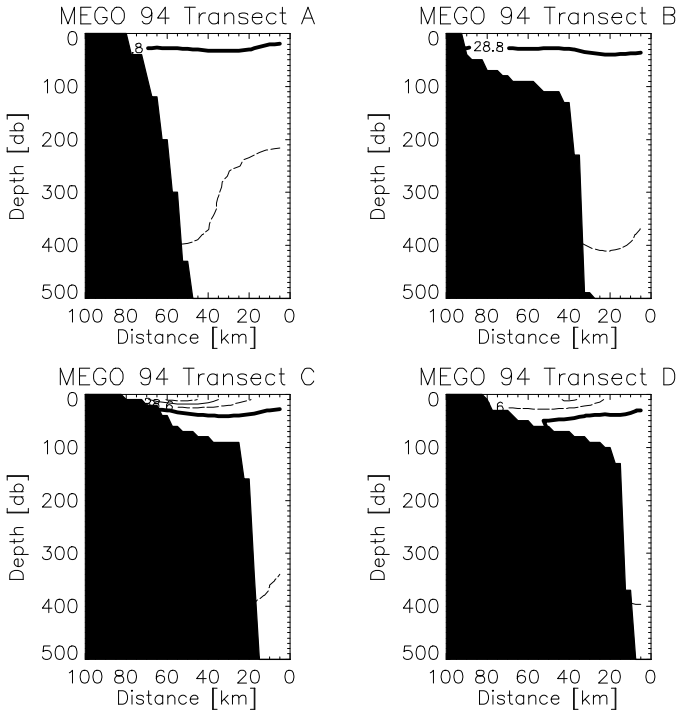

Figure 6-73 Density (sigma theta) transects for MEGO 94 for the standardized analysis with the first six modes.

Finally, we shall now introduce another type of plots, aimed to get a deeper insight into the behaviour of the non-standardized EOF model, which produces such large errors at certain depth levels. We have chosen three transects of CTD casts, which clearly show the EOF extrapolation behaviour under three different upper layer conditions. Their location has been presented in Figure 6-28 with the density distribution at 10 m.

The following two Figures correspond to transects C and G respectively, each transect has eight CTD casts and are presented ordered from open sea (the deeper ones) to the shelf (the shallower ones). Thus, each one of these Figures has eight plots with two lines, full and dashed, which in turn represent the data density profile from the CTD casts and the EOF profile considering the first six modes. When the casts are shallower than 500 m, a straight line is defined from the shallower bottom depth towards the density value at 10 m, and this value is kept constant for the rest of the profile. This feature produces a step-like structure in each one of the shallow casts (for example, from the third frame onwards in the following Figure). On the other hand, the dashed line goes

all the way down to 500 m in order to visualize one of the applications of the EOF approach: the extrapolation of shallow profiles. [This feature will be essential for geostrophic estimates on the shelf, as it is explained in the corresponding section in Chapter 7.]

Transect C is located to the north of the domain, in an area with little variability, both in the horizontal and in the vertical (Figure 6-74). The vertical density gradients are very small, the EOF profiles with the non-standardized analysis reproduce very well the data, with differences ranging between –0.01 and 0.015, and the extrapolated curves seem reasonable.

The above conditions are no longer met in transect G (Figure 6-75), located in an area where the influence of the Ebro Delta is important. While in the deeper casts vertical gradients are small, they become more important as the Ebro Delta draws nearer. The strong near-surface gradients determine the amplitude values associated to each EOF in a way such as to produce a good fit in the uppermost layer, but generates a profile that deviates from the data at deeper levels, becoming totally unrealistic when values are extrapolated.

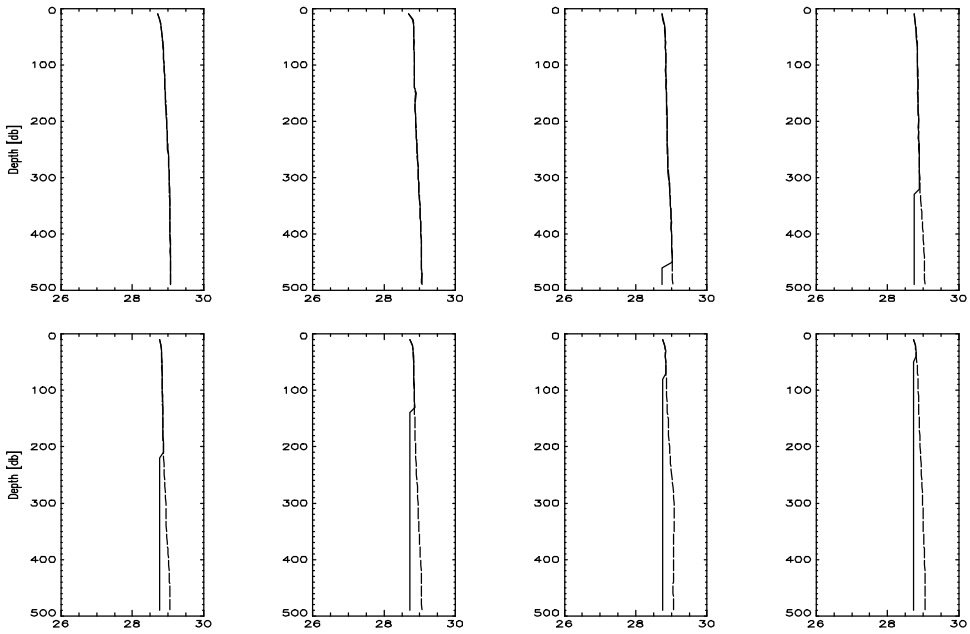

Figure 6-74 MEGO 94 Transect C CTD density profiles, refer to Figure 6-28 for geographic location. Full lines represent the CTD data, while the dashed lines represent the EOF profile with six modes, which can be extended below the cast depth. The step-like structure marks the bottom depth of the corresponding cast.

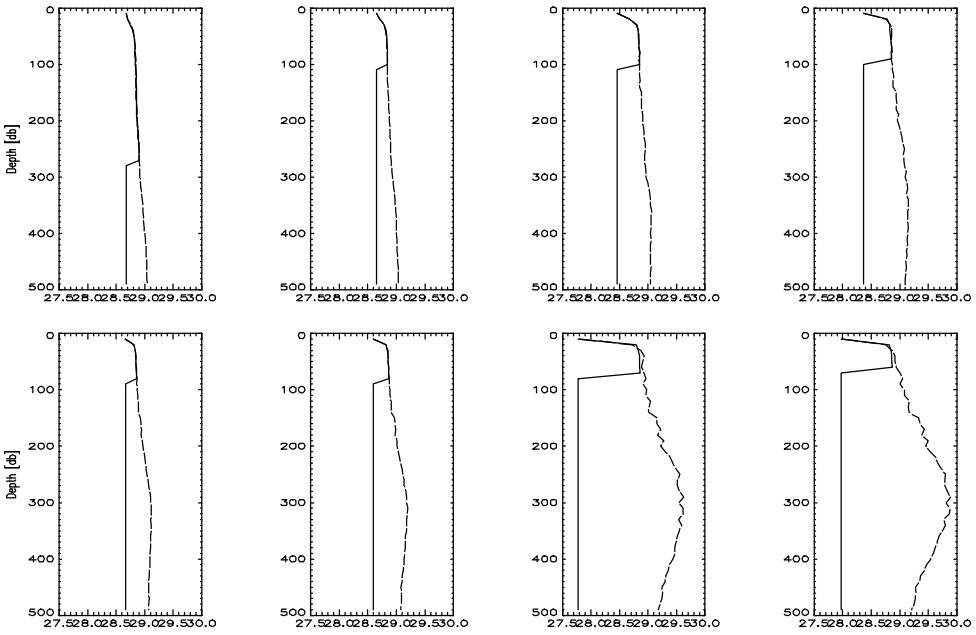

Figure 6-75 MEGO 94 Transect G CTD density profiles. Refer to Figure 6-28 for geographic location. X axis range = [27.5 - 30]

These results reflect that the open sea vertical structure can not be considered to represent the conditions on the shelf. As mentioned in the data chapter, the average and standard deviation profiles obtained with the deep casts differ significantly from the ones obtained with all the available data. And there is also the condition of very little variability both on the horizontal and in the vertical with the deep casts, which then implies that they might have redundant spatial information.